

# On coarse-graining by the Inverse Monte Carlo method: Dissipative Particle Dynamics simulations made to a precise tool in soft matter modeling

Alexander P. Lyubartsev<sup>[a]</sup>, Mikko Karttunen<sup>[b]</sup>, Ilpo Vattulainen<sup>[c]</sup>, and Aatto Laaksonen<sup>[a]</sup>  
<sup>[a]</sup> *Division of Physical Chemistry, Arrhenius Laboratory, Stockholm University, S-106 91, Stockholm, Sweden*  
<sup>[b]</sup> *Biophysics and Statistical Mechanics Group, Laboratory of Computational Engineering, Helsinki University of Technology, P. O. Box 9400, FIN-02015 HUT Helsinki, Finland*  
<sup>[c]</sup> *Laboratory of Physics and Helsinki Institute of Physics, Helsinki University of Technology, P. O. Box 1100 FIN-02015 HUT, Helsinki, Finland*

We present a promising coarse-graining strategy for linking micro- and mesoscales of soft matter systems. The approach is based on effective pairwise interaction potentials obtained from detailed atomistic molecular dynamics (MD) simulations, which are then used in coarse-grained dissipative particle dynamics (DPD) simulations. Here, the effective potentials were obtained by applying the Inverse Monte Carlo method [Lyubartsev & Laaksonen, Phys. Rev. E, **52**, 3730 (1995)] on a chosen subset of degrees of freedom described in terms of radial distribution functions. In our first application of the method, the effective potentials were used in DPD simulations of aqueous NaCl solutions. With the same computational effort we were able to simulate systems of one order of magnitude larger as compared to the MD simulations. The results from the MD and DPD simulations are found to be in excellent agreement.

**Keywords:** Computer simulations, atomistic force fields, effective potentials, dissipative particle dynamics, mesoscale modeling, coarse-graining

## I. INTRODUCTION

Classical molecular dynamics computer simulations with site-site pair potentials can currently be run for molecular systems consisting of the order of  $10^4$  atoms, corresponding typically to a system size of 50–60 Å. Corresponding time scales using the same approach are typically of the order of 10 ns. This may be enough for simulations of isotropic liquids of simple molecules, while for many complex systems the requirements for the length and time scales are much more extensive.

The restrictions of the detailed all-atom description are especially severe in soft matter systems such as biomembranes and polyelectrolytes, although these are just two examples of the diversity of soft materials. This is mainly due to a wide range of time and length scales associated with these systems, and it is obvious that these problems become particularly pronounced in studies of dynamic processes which usually take place under hydrodynamic conditions. The primary aim in coarse-graining is to build a bridge between different time and length scales. Although there is no unique way to do this, the coarse-graining procedure always leads to a reduction of the number of degrees of freedom and thus alleviates the computational burden. The challenge is to establish systematic coarse-graining schemes that allow one to develop simplified model systems in terms of the information extracted from the underlying microscopic systems. Thus far, various approaches have been used to coarse-grain atomic and molecular systems. Below, we will briefly discuss some of them.

As a relatively generic approach, the dissipative particle dynamics (DPD) [1, 2, 3] has been used to study coarse-grained particle and polymeric systems, see e.g. Ref. [4] for a review. In our approach we use DPD as a thermostating method which is discussed in more detail in the following sections. To mention other relatively generic approaches, Flekkøy et al. [5, 6]

have recently introduced a hybrid method to combine particle and continuum level descriptions. This framework allows a derivation of the DPD model and in practice uses a Voronoi tessellation based technique for simulations of coarse-grained particles at different levels. Another very promising approach was presented by Malevanets and Kapral [7, 8] who proposed a framework to couple a molecular level description with a mesoscale treatment of solvent that conserves hydrodynamics. This approach seems particularly appealing for studying dilute systems with hydrodynamics.

A lot of impetus for multiscale modeling has come from polymer research due to both fundamental and practical reasons. Akkermans and Briels [9] applied a projector operator formalism based approach to coarse-grain polymer chains using a microscopic model as a starting point. Their approach is appealing and deserves further studies since it accounts for the fluctuating forces at the coarse-grained level. Bolhuis et al. [10, 11] used the Ornstein-Zernike equation [12] with a hypernetted-chain closure to invert the pair correlation function in order to derive effective pair potentials for neutral polymers in a solution. The coarse-grained polymers were represented as soft colloidal particles. Their approach is based on a theorem proved by Henderson in 1974 [13] that stipulates a unique, point-to-point correspondence between pair potentials and radial distribution functions  $g(r)$ . The importance of this theorem becomes clear when one notices that for any  $g(r)$  under given conditions there is a unique pair potential that includes corrections from the many-body interactions, and that by definition the pair potential then yields the original  $g(r)$ . The problem is thus reduced to inverting the  $g(r)$  obtained from a microscopic model – how to obtain a coarse-grained model from that information lies at the heart of the problem of coarse-graining. At the representational level the soft ellipsoid model for polymer melts by Murat and Kremer [14] is very close to the one of Bolhuis et al. [10, 11], but instead of using the pair correlation function Murat and Kremer

base their approach on separating the free energy into intra- and interchain parts. In an attempt to model more realistic systems, Reith et al. [15] introduced a coarse-graining procedure that starts from a detailed chemical description of a polymer. In order to obtain a coarse-grained approach, a simplex algorithm based optimization is performed to obtain a coarse-grained force field. The structural features produced by this approach are in good agreement with experimentally observed ones. For a more complete overview of the current coarse-graining approaches, see e.g. Ref. [16] and references therein.

Our approach is also based on inverting the radial distribution function but instead of the integral equation based approach of Bolhuis et al. [10, 11] we use the inverse Monte Carlo procedure of Lyubartsev and Laaksonen [17] which will be discussed in the following section. This *systematic* coarse-graining method is then combined with a *momentum conserving* dissipative particle dynamics (DPD) thermostat. Our approach consists of three conceptually simple steps. First, we use a detailed atomistic description and perform MD simulations. From these simulations we compute radial distribution functions  $g(r)$  between different atoms, molecules, or molecular groups. Second, we apply the Inverse Monte Carlo [17] procedure to invert the radial distribution functions. This yields effective interaction potentials  $V^e(r)$  between the selected interaction sites. Finally, we employ these effective, coarse-grained potentials in the DPD algorithm to study the large-scale properties of systems in question. Note that since DPD satisfies momentum conservation, the present approach allows studies of a given system with full hydrodynamics.

Preliminary results of this work were recently reported in Ref. [18], in which we presented only the most essential ideas of this approach. Our aim in this article is to provide one with a comprehensive discussion of issues related to coarse-graining and mesoscopic simulations in terms of the DPD method. In particular, we discuss in detail how atomistic MD simulations can be coupled to DPD by the Inverse Monte Carlo method. To this end, we use NaCl as our model system. Even in this simple system, and with a very modest degree of coarse-graining, we obtain a computational speed-up of one order of magnitude. Our procedure is well-defined and truly allows easy and controllable tuning of the level of coarse-graining. Finally, we show through coarse-grained DPD simulations that this approach is physically sound and provides results in excellent agreement with the MD simulations and experiments.

This paper is organized as follows. First, in Sect. II, we describe the methods: The Inverse Monte Carlo procedure and the DPD algorithm. In Sect. III we present the results and finally, in Sect. IV, we discuss the results and some general aspects related to the general applicability of the method.

## II. METHODS AND MODELS

As discussed in the Introduction, detailed atomistic simulation techniques are suitable for studies of microscopic features of soft matter systems, e.g. the excited states of a chro-

mophore where the time scales of interest are within a few hundreds of femtoseconds. For studies of systems that are characterized by large time and length scales, such as a protein in water solution over tens or hundreds of nanoseconds, however, atomistic simulation techniques are not very feasible. Our aim in this section is to discuss ways how this problem can be resolved by coarse-graining microscopic systems. In particular, we concentrate on an approach based on solving the “inverse problem” which yields effective interaction potentials which in turn can be coupled to mesoscopic simulation techniques such as the dissipative particle dynamics method discussed below. Full details of the methods can be found in Refs. [17] and [19, 20], respectively.

### A. The Inverse Problem in statistical mechanics

In the standard statistical mechanical description of soft matter systems one begins from a formulation of a model, which is usually given in terms of a Hamiltonian or interaction potentials between atoms and molecules. When a Hamiltonian is specified, one can use different numerical methods to compute canonical averages such as energies, distribution functions, and response functions which can be compared with experiments. As one has an explicit expression for the canonical averages, their calculation is in principle a fairly straightforward task, although in many cases it may be computationally a very demanding one.

Occasionally one is interested in the solution of the inverse problem, i.e., how to deduce information about molecular interactions from the canonical averages which may be known from experiments. More specifically, the question is how to reconstruct the Hamiltonian based on results for the canonical averages. Many experimental properties can be chosen as a starting point to this end. Among the most important ones for the liquid state are the radial distribution functions  $g(r)$ , which may be known from the structure factor measurements using X-ray or neutron scattering [12]. In 1974, Henderson proved a theorem [13] stipulating a unique, point-to-point correspondence between pair potentials and radial distribution functions. In essence it states that for a given system under given conditions of temperature and density, two pair potentials which give rise to the same radial distribution function cannot differ more than by an additive constant. As this constant can be defined from the condition that the interaction potential tends to zero at an infinite distance, the potential is uniquely defined. In practice the solution of an inverse problem is not a straightforward calculation, however, since  $g(r)$  does not provide one with a formal expression for the potential. Therefore, some special techniques are required for the solution of the inverse problem.

In 1988, McGreevy and Pusztai suggested a Reverse Monte Carlo (RMC) method in which the starting point for a simulation was the radial distribution function [21]. In this method, Monte Carlo simulations are carried out without any prior knowledge of the interaction potential to fit  $g(r)$  that serves as an input. The set of configurations obtained in RMC may be used for further structural analysis, for example for calcula-

tion of three-dimensional spatial or orientational correlations. However, as the interaction potential is not recovered, the inverse problem is not solved completely, and it is not possible to calculate thermodynamical or dynamical properties using this approach. For the same reason this approach is not suitable for the development of coarse-grained models.

In another approach, Reatto et al. [22] used the Hypernetted Chain (HNC) approximation to solve the inverse problem. This and similar approaches, based on some closure of the Ornstein-Zernike equation, have been used in a number of works during the last decade to compute interaction potentials from radial distribution functions [23, 24]. It should be noted, however, that computations within the HNC theory are feasible only for relatively simple models. Moreover, although yielding sometimes very accurate results [25], the HNC theory is not an exact mathematical solution of the statistical-mechanical problem, and its accuracy should be investigated carefully in every specific case. Other works devoted to the inverse problem are listed in Refs. [26, 27, 28].

A practical way to solve the inverse problem has been suggested by Lyubartsev and Laaksonen [17]. This is the method we will concentrate on in the following, and we will use it to compute effective potentials from radial distribution functions obtained from detailed MD simulations. The effective potentials then allow us to study the large-scale properties of a given model system through coarse-grained DPD simulations.

### B. The Inverse Monte Carlo Method – A Simple Case

To illustrate the Inverse Monte Carlo method, we consider the case of a single-component system consisting of identical particles with pairwise interactions. The general case of a multicomponent system is a straightforward extension of it. The Hamiltonian for this system is given as

$$H = \sum_{i,j} V(r_{ij}); \quad (1)$$

where  $V(r_{ij})$  is the pair potential and  $r_{ij}$  is the distance between the interaction sites  $i$  and  $j$ . Let us assume that we know the radial distribution function  $g(r_{ij})$ . Our aim is now to find the corresponding interaction potential  $V(r_{ij})$ .

Let us introduce the following grid approximation to the Hamiltonian,

$$\tilde{V}(r) = V(r) - V \quad (2)$$

for

$$r - \frac{1}{2M} < r < r + \frac{1}{2M} \quad \text{and} \quad r = (0.5) r_{\text{cut}} = M; \quad (3)$$

where  $M = 1; \dots; M$ , and  $M$  is the number of grid points within the interval  $[0; r_{\text{cut}}]$ , and  $r_{\text{cut}}$  is a chosen cut-off distance. Then, the Hamiltonian in Eq. (1) can be rewritten as

$$H = \sum_{i,j} V(S); \quad (4)$$

where  $S$  is the number of pairs with interparticle distances inside the  $i$ -slice. Evidently,  $S$  is an estimator of the radial distribution function:  $hS_i = 4 \pi r^2 g(r) N^2 = (2V)$ . The average values of  $S$  are some functions of the potential  $V$  and can be written as an expansion

$$hS_i = \sum \frac{\partial hS_i}{\partial V} V + O(V^2); \quad (5)$$

The derivatives  $\partial hS_i / \partial V$  can be expressed using exact statistical mechanics relationships [17]

$$\begin{aligned} \frac{\partial hS_i}{\partial V} &= \frac{\partial}{\partial V} \frac{\sum_R \frac{d g(S)}{d q} \exp(-\sum_P K(S(q)))}{\sum_R \exp(-\sum_P K(S(q)))} \\ &= \frac{hS_i - hS_i}{k_B T}; \end{aligned} \quad (6)$$

Equations (5) and (6) allow us to find the interaction potential  $V$  iteratively from the radial distribution functions  $hS_i$ . Let  $V^{(0)}$  be a trial potential for which a natural choice is the potential of mean force (PMF)

$$V^{(0)} = -k_B T \ln g(r); \quad (7)$$

By carrying out standard Monte Carlo simulations, one can evaluate the averages  $hS_i$  and their deviations from the reference values  $S_i$  defined from the given radial distribution function as  $hS_i^{(0)} = hS_i^{(0)} / S_i$ . By solving the system of linear equations [Eq. (5)] with coefficients defined by Eq. (6), and omitting terms  $O(V^2)$ , we obtain corrections to the potential  $V^{(0)}$ . The procedure is then repeated with the new potential  $V^{(1)} = V^{(0)} + V^{(0)}$  until convergence is reached. The whole procedure resembles a solution of a multidimensional non-linear equation using the Newton-Raphson method.

If the initial approximation of the potential is poor, some regularization of the iteration procedure is needed. In this case we multiply the required change of the radial distribution function by a small factor that is typically between 0 and 1. By doing so, the term  $O(V^2)$  in Eq. (5) can be made small enough to guarantee convergence of the whole procedure, although the number of iterations will increase.

The above algorithm has also the advantage that it provides us with a method to evaluate the uncertainty of the inverse procedure. The radial distribution function has normally some uncertainty. An analysis of the eigenvalues and eigenvectors of the matrix in Eq. (6) allows one to make conclusions of which changes in  $g(r)$  correspond to which changes in the potential. For example, eigenvectors with eigenvalues close to zero correspond to changes in the potential which have almost negligible effect on the radial distribution function. The presence of these small eigenvalues makes the inverse problem not well-defined, however. In some cases, such as for liquid water, that may pose serious problems in the inversion procedure [29].

It is instructive to note a relation between the present approach and the renormalization group Monte Carlo method [30, 31] used to study phase transitions in lattice models (e.g.,

polymer models and Ising models for ferromagnets) as well as in the quantum field theory. The renormalization procedure introduces a scale change in the system. During this procedure one consecutively obtains a more and more coarse-grained description of the system. Equations (5) and (6) were in fact used by Swendsen et al. [30, 31] to describe how the parameters of a Hamiltonian change during the renormalization procedure. It now appears that the applications of this method are more general than the original lattice systems near a phase transition, and cover even soft matter problems allowing us to “renormalize” Hamiltonians of molecular systems in such a way that only the degrees of freedom of primary interest are kept in the coarse-grained system.

### C. Dissipative Particle Dynamics (DPD)

Dissipative particle dynamics was introduced in 1992 by Hoogerbrugge and Koelman for simulations of hydrodynamic phenomena in complex fluids [1, 2]. The original formulation did not obey detailed balance, though, and in 1995 Español and Warren [3] formulated a new DPD algorithm which they showed to be fully consistent with statistical mechanics. This algorithm is nowadays known as DPD. In the following we present the basic DPD formalism and discuss some of its features that are relevant to the present work.

In the basic formulation of DPD, the interactions are pairwise additive and the force exerted by particle  $j$  on particle  $i$  is given as a sum of conservative, dissipative, and random forces through  $\mathbf{F}_{ij} = \mathbf{F}_{ij}^C + \mathbf{F}_{ij}^D + \mathbf{F}_{ij}^R$ , respectively. These forces are typically given as

$$\mathbf{F}_{ij}^C = F_{ij}^{(c)}(\mathbf{r}_{ij}) \mathbf{e}_{ij}; \quad (8)$$

$$\mathbf{F}_{ij}^D = -\gamma^D(\mathbf{r}_{ij}) (\mathbf{v}_{ij} \cdot \mathbf{e}_{ij}) \mathbf{e}_{ij}; \quad (9)$$

$$\mathbf{F}_{ij}^R = \gamma^R(\mathbf{r}_{ij}) \boldsymbol{\xi}_{ij} \mathbf{e}_{ij}; \quad (10)$$

where  $\mathbf{r}_{ij} = \mathbf{r}_i - \mathbf{r}_j$  is the position vector connecting two particles,  $r_{ij} = |\mathbf{r}_{ij}|$  is the interparticle distance,  $\mathbf{e}_{ij} = \mathbf{r}_{ij}/r_{ij}$  is the corresponding unit vector, and  $\mathbf{v}_{ij} = \mathbf{v}_i - \mathbf{v}_j$  is the relative velocity of particles  $i$  and  $j$ . The terms  $\boldsymbol{\xi}_{ij}$  are symmetric random variables with zero mean and unit variance, and are independent for different pairs of particles and different times. The conservative force is essentially given by  $F_{ij}^{(c)}(r_{ij})$ . Constants  $\gamma^D$  and  $\gamma^R$  give the amplitudes of the dissipative and random forces, respectively, and  $\gamma^D$  and  $\gamma^R$  are the corresponding weight functions.

Let us now return to the different forces. The DPD formulation does not specify the form of the conservative force. The most common choice in standard DPD simulations is  $F_{ij}^{(c)}(r_{ij}) = \epsilon_{ij} (1 - r_{ij}/r_c)$  for  $r \leq r_c$  and  $F_{ij}^{(c)}(r_{ij}) = 0$  otherwise. In other words, the conservative force is derived from a soft pair potential  $U = \epsilon_{ij} (1 - r_{ij}/r_c)^2/2$ , where  $r_c$  is the cutoff distance. Interactions between different types of coarse-grained particles can then be described by varying the amplitude of the conservative interaction  $\epsilon_{ij}$  [32].

The above is the preferred formulation for the conservative force when generic, simple, and soft interactions are ade-

quate. It was shown by Forrest and Suter in 1995 that coarse-graining of molecular representation leads to this type of softening [33]. However, in many cases this formulation is of too generic nature. Although it is possible to use mean field theories such as the Flory-Huggins theory for polymers to find the amplitudes for the conservative forces between different types of particles [32], there are cases where this approach does not retain enough information about the actual character of the different atoms, molecules, or interactions (see discussion below).

The weight functions for the dissipative and random forces,  $\gamma^D$  and  $\gamma^R$ , cannot be chosen arbitrarily. This is easy to understand by the intuitive argument that the thermal heat generated by the random force must be balanced by dissipation. Español and Warren [3] studied this situation analytically and derived a fluctuation-dissipation relation connecting the weight functions and amplitudes of the dissipative and random forces via

$$\gamma^D(r_{ij}) = \gamma^R(r_{ij})^2 \quad \text{and} \quad \gamma^2 = 2 k_B T; \quad (11)$$

These conditions guarantee convergence to the canonical ensemble as required. It is important to notice that  $\gamma^D$  and  $\gamma^R$  are completely decoupled from the conservative part. In other words, we can consider the DPD algorithm as a momentum conserving thermostat for an arbitrary conservative potential. This is in fact the way how we apply the DPD algorithm in our coarse-grained simulations: The conservative potential is defined through the Inverse Monte Carlo procedure and then used in the DPD algorithm.

Finally, to study the dynamics of the system one needs to evolve the system in time. In DPD this is simply done by integrating the Newton's equations of motion. In our simulations we used a velocity-Verlet based algorithm adapted for DPD (sometimes called DPD-VV) [19, 20].

### D. Combining MD and DPD

With the above definitions we now have all the tools for coarse-graining. We remove fast internal and orientational degrees of freedom from all water molecules, and represent water molecules as one-site particles interacting with other water particles and ions by spherically symmetric potentials. In comparison to the original all-atom model, we have approximately one third of the degrees of freedom left. This can be interpreted as intermediate level of coarse-graining.

Without any loss of generality we can choose the weight functions to be of the standard form  $\gamma^R(r_{ij}) = 1 - r_{ij}/r_c$  as discussed above. This choice has been made invariably in DPD simulations. Since the Inverse Monte Carlo procedure provides us with the effective potentials, thus yielding us  $F_{ij}^C(r)$ , the only task left is to ensure that the MD and DPD systems correspond to each other. In this study, that was done by adjusting the amplitude of the dissipative force which determines the dissipation rate in the DPD system. Here,  $\gamma^D$  was determined by requiring the short-time decay of the single-

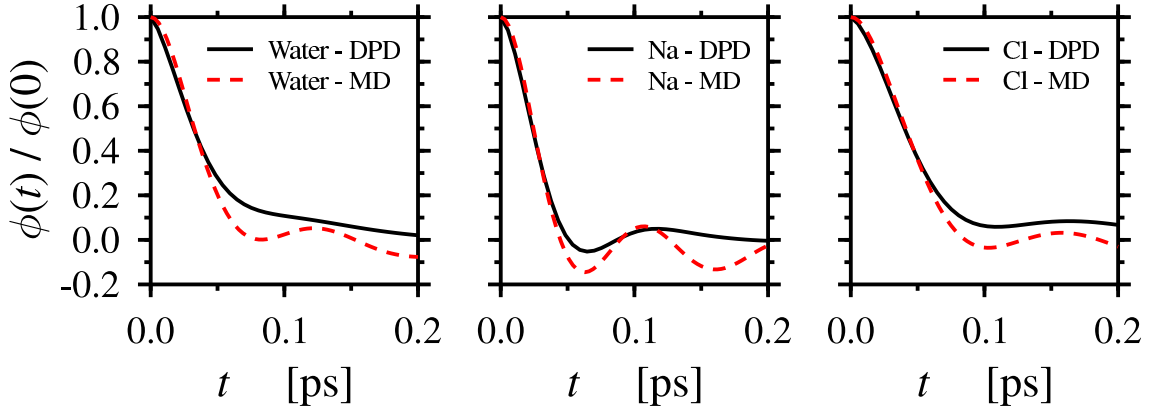


FIG. 1: The decay of the single-particle velocity autocorrelation function  $\phi(t)$  at early times. Results shown here are for water,  $\text{Na}^+$  and  $\text{Cl}^-$  ions. As the data illustrates, the early-time decay of  $\phi(t)$  is essentially identical between MD and DPD simulations for  $\gamma = 0.72$  used in the DPD simulations.

particle velocity autocorrelation function

$$\phi(t) = \langle \mathbf{v}_i(t) \cdot \mathbf{v}_i(0) \rangle / \langle \mathbf{v}_i^2 \rangle \quad (12)$$

to be approximately the same in both MD and DPD systems as shown in Fig. 1. It shows how the early-time decay of  $\phi(t)$  can be matched, leading to a value of  $\gamma = 0.72$  for the DPD model. The long-time behavior of the velocity autocorrelation function between MD and DPD is different, however. This is an obvious result since some microscopic degrees of freedom have been coarse grained and thus effects due to hydrogen bonds, for example, are *implicitly* included in the effective interactions. This leads to an enhanced diffusion rate at intermediate times, and is demonstrated in Fig. 1 as a positive tail for the DPD particles.

This approach is meaningful since (i) it makes sure that the early-time dynamics is described properly, while (ii) it does not fix the tracer diffusion coefficient. One should notice that the tracer diffusion coefficient is an integral over the velocity correlation function over long times, and in hydrodynamic systems the long-time tail is important. With this choice, we can assume the diffusion coefficient to be an independent quantity so that its behavior, found by DPD, can be compared with both MD simulations and experiments. Fixing  $\gamma$  thus determines the transport properties of the system.

### III. RESULTS

#### A. Constructing the potentials

One of the typical simplifications used in molecular simulations is the replacement of solvent molecules by continuum media. For example, in the primitive electrolyte model, ions in water are substituted by charged spheres moving in dielectric media with the dielectric constant set to about 80. This is a serious simplification at small distances (a few ångströms) where it is impossible to define a dielectric constant. Besides this, in the primitive electrolyte model the ion radius is an adjustable parameter without any clear physical meaning. A bet-

ter model for effective ion-ion interactions in an aqueous solution must take into account the solvation structure around the ions. Practically, effective solvent-mediated ion-ion potentials may be constructed by the Inverse Monte Carlo method from ion-ion radial distribution functions generated in high-quality all-atomic molecular dynamics simulations [17, 25, 34]. This is the approach we used in obtaining the effective potentials.

The MD simulations were performed in the NVT ensemble using the flexible SPC water model [35] and Smith–Dang parameters for  $\text{Na}^+$  and  $\text{Cl}^-$  ions [36], i.e., the Lennard-Jones parameters for the sodium ions were  $\sigma = 2.35 \text{ \AA}$  and  $\epsilon = 0.544 \text{ kJ/mol}$ , and for chloride  $\sigma = 4.4 \text{ \AA}$  and  $\epsilon = 0.419 \text{ kJ/mol}$ . In the results reported here we set the temperature to 300 K. The electrostatic interactions were taken into account by Ewald summation. Other simulation details are described in Refs. [17, 34]. From the MD simulations, the radial distribution functions between different pairs of particles were calculated and fed as an input in the Inverse Monte Carlo procedure. The results are shown in Figs. 2 and 3.

Figure 2 shows effective potentials between water molecules, presented as one-center particles, and between other water molecules and ions. For comparison, water-water effective potential calculated from MD simulations for *pure* water is also displayed. It is interesting to note that the presence of ions has practically no effect on the water-water effective potential.

Figure 3 displays the effective potentials between the ions. They are compared to the effective potentials calculated without water [17, 34]. The effective potentials are very similar in the two cases both of them having an oscillating character with one or two oscillations. The potential approaches the primitive model potential with dielectric constant close to 80. At distances above  $10 \text{ \AA}$  the effective potential coincides almost perfectly with the Coulombic potential.

Within the inverse Monte Carlo procedure, calculation of effective potentials without water is much easier than in the presence of water. On the other hand, the presence of particles representing water is necessary in DPD simulations. Our test studies have shown that while the use of effective potentials

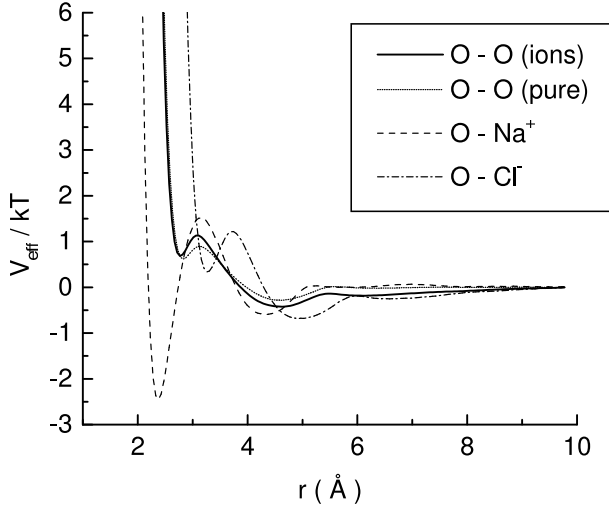


FIG. 2: Effective potentials for coarse-grained water in NaCl solution. Thin dotted line is water-water effective potential in pure water. “O” refers to an oxygen atom in the water molecule.

calculated without water may give qualitatively satisfactory results, inclusion of water in the Inverse Monte Carlo simulations essentially leads to an improvement of results, especially in the case of dynamical properties.

It is worth pointing out that the effective potential differs from the potential of mean force defined as  $\beta P M F = -k_B T \ln g(r)$ , which corresponds to the Kirkwood approximation for the  $n$ -particle correlation function. The potential of mean force is screened by the other ions in a system and decays as  $(1/r)e^{(r-r_D)}$ , i.e., not as the  $1/r$  Coulombic potential. The potential of mean force is therefore not a very suitable choice to present ion-ion interactions within a continuum solvent model at finite ion concentrations even in a coarse-grained solvent system. The effective potentials include a contribution from Coulombic forces, however.

### B. Coarse-grained simulations

In our first paper using this approach [18], we showed that the radial distribution functions computed from the coarse-grained DPD simulations for the pairs between the  $\text{Na}^+$  and  $\text{Cl}^-$  ions agreed with those obtained from the all-atom MD simulations. In addition to the static properties, the diffusion coefficients were shown to be in good agreement between the MD and DPD results at various NaCl concentrations between 0.5 M and 4.1 M. What makes those results very interesting is the fact that, for all the DPD simulations, we used the effective potentials obtained at one single NaCl concentration only. In that case, the effective potentials were obtained from MD simulations at a salt concentration of 0.87 M and then used in DPD simulations for various salt concentrations between 0.5 M and 4.1 M. When compared with MD simulations, the agreement was found to be excellent. Here, we present results for static correlations, coordination numbers, velocity auto-correlation functions, and viscosity.

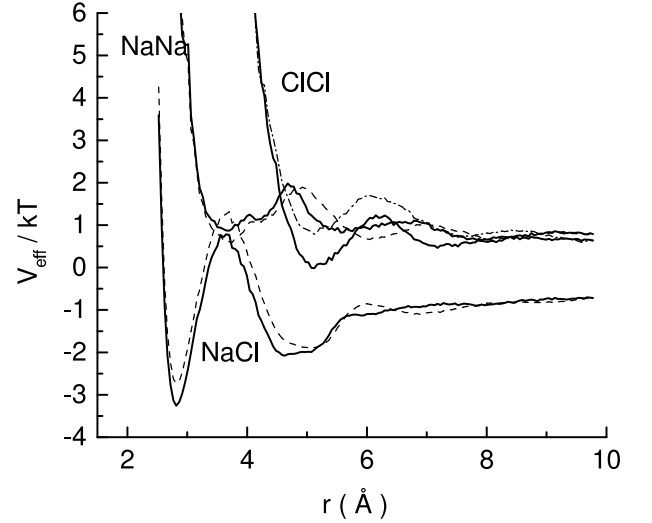


FIG. 3: Ion-ion effective potentials in aqueous solution. Solid lines describe potentials in presence of one-site water molecules (this work), while dashed lines are for effective potential without water from Ref. [34].

|      | molarity:       | 0.55 M | 0.87 M | 2.2 M | 4.1 M |
|------|-----------------|--------|--------|-------|-------|
| MD:  | $\text{Na}^+$ : | 5.8    | 5.5    | 5.42  | 5.3   |
|      | $\text{Cl}^-$ : | 6.9    | 6.8    | 6.9   | 7.1   |
| DPD: | $\text{Na}^+$ : | 5.67   | 5.66   | 5.55  | 5.40  |
|      | $\text{Cl}^-$ : | 6.91   | 6.96   | 6.97  | 7.00  |

TABLE I: Coordination numbers obtained from MD and DPD simulations at various salt concentrations. The error bars for both cases are  $\pm 0.05$ . The MD data is from Ref. [39].

It is important to notice that due to the self-consistency conditions for the effective potentials, the DPD simulations will always produce the correct pair correlation behavior at the point in phase space where the effective interactions were determined in the first place. As an example, this is demonstrated in Fig. 4 for all different kinds of pairs of particles studied in this work. It is very relevant to ask, however, how the effective interactions change when system variables such as the salt concentration or the temperature of the system change. We have explored this matter through combined MD and DPD simulations and found that for a wide range of salt concentrations in the present system it is *not* necessary to recalculate the effective potentials. This is demonstrated by the data in Table I which compares the coordination numbers obtained from DPD and MD simulations for  $g(r)$ . In the DPD simulations we have again used the effective potentials obtained at 0.87 M. We find that both MD and DPD follow the same qualitative behavior. For sodium the coordination number decreases with increasing salt concentration whereas for chloride we find an opposite trend. Furthermore, the quantitative agreement between the MD and DPD results is remarkably good.

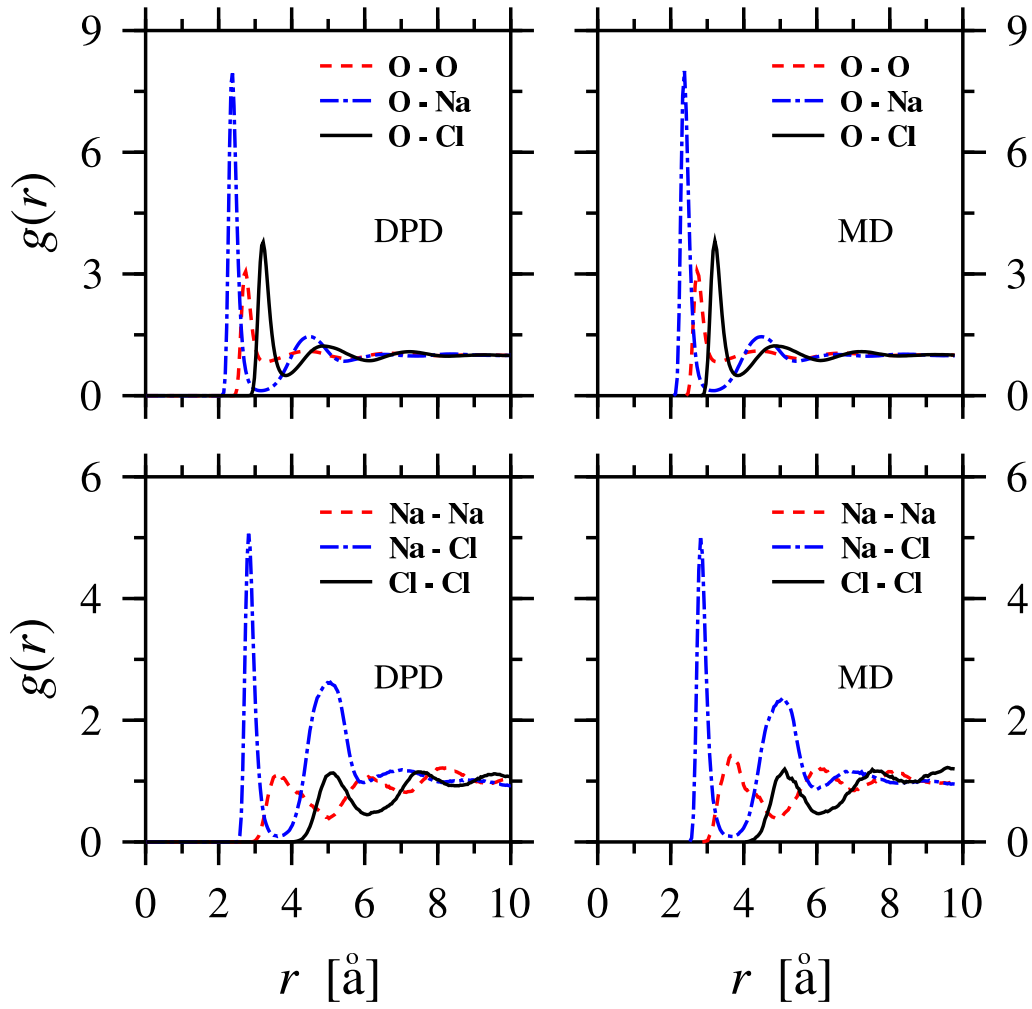


FIG. 4: Radial distribution functions  $g(r)$  for different pairs of particles in the aqueous NaCl system studied by both DPD (shown on the left) and MD (on the right). The studies were made at a salt concentration of 0.87 M. “O” refers to the oxygen atom in the water molecule. Note the agreement between MD and DPD results.

Our finding that the effective interactions depend only weakly on thermodynamic conditions is also supported by the present results for shear viscosity (see below) and earlier studies of the same system for tracer diffusion [18]. In Ref. [18], we found that DPD simulations with effective potentials yielded tracer diffusion coefficients in good agreement with MD simulations. Further support for this result is given by previous work [25, 34], where the dependence of effective potentials on the salt concentration was studied in detail. It was found that effective potentials depend very little on the salt concentration: An increase in salt concentration leads to a slow decrease in the dielectric permittivity.

Our results thus suggest that the effective interactions change only slightly when the system parameters are varied, as is here the case for salt concentration. However, while this result holds true in the present system for an aqueous solution of monovalent ions, the generality of this finding remains an open question. Further studies of divalent systems and more complex molecules, among others, are therefore called for.

Next, we determined the shear viscosity using a Green-Kubo relation. As with the other quantities, the shear viscosity should be compared to results from the MD simulations. However, since the shear viscosity coefficient is a collective quantity, meaning that all particles in a system give rise to a single sample, an accurate determination of the shear viscosity coefficient through MD simulations is both difficult and very time-consuming. Thus it was not done in the present case, and as a matter of fact, to the best of our knowledge, there are no published reports of MD simulations of shear viscosity in NaCl solutions. Thus, we compare our DPD data to experimental results [37] instead. The results shown in Fig. 5 indicate that the qualitative behavior of the shear viscosity coefficient obtained through DPD simulations is in good agreement with the experiments. This result is truly remarkable as it shows that both the equilibrium (static) and dynamic behavior of the system are properly described by the coarse-grained approach. This provides us with strong support that the present approach of coarse graining an MD system and applying the obtained effective interactions in DPD simulations





### Acknowledgments

This work has been supported by the Swedish Science Council (A.P.L. and A.L.) and the Academy of Finland

(M.K.). Further support has been obtained from the Academy of Finland through its Centre of Excellence Program (I.V.) and from the Finnish Academy of Science and Letters (I.V.).

- 
- [1] Hoogerbrugge, P. J.; Koelman, J. M. V. A. *Europhys. Lett.* **1992**, *19*, 155–160.
  - [2] Koelman, J. M. V. A.; Hoogerbrugge, P. J. *Europhys. Lett.* **1993**, *21*, 363–368.
  - [3] Español, P.; Warren, P. *Europhys. Lett* **1995**, *30*, 191–196.
  - [4] Warren, P. B. *Curr. Opin. Coll. Interf. Sci.* **1998**, *3*, 620–624.
  - [5] Flekkøy, E. G.; Coveney, P. V. *Phys. Rev. Lett.* **1999**, *85*, 2522.
  - [6] Flekkøy, E. G.; Wagner, G.; Feder, J. *Europhys. Lett.* **2000**, *52*, 271–276.
  - [7] Malevanets, A.; Kapral, R. *J. Chem. Phys.* **1999**, *110*, 8605–8613.
  - [8] Malevanets, A.; Kapral, R. *J. Chem. Phys.* **2000**, *112*, 7260–7269.
  - [9] Akkermans, R. L. C.; Briels, W. J. *J. Chem. Phys.* **2000**, *113*, 6409–6422.
  - [10] Louis, A. A.; Bolhuis, P. G.; Hansen, J. P.; Meijer, E. P. *Phys. Rev. Lett.* **2000**, *85*, 2522.
  - [11] Bolhuis, P. G.; Louis, A. A.; Hansen, J. P.; Meijer, E. P. *J. Chem. Phys.* **2001**, *114*, 4296–4311.
  - [12] Hansen, J. P.; McDonald, I. R. *Theory of simple liquids*; Academic press: London, 1986.
  - [13] Henderson, R. L. *Phys. Lett.* **1974**, *49A*, 197–198.
  - [14] Murat, M.; Kremer, K. *J. Chem. Phys.* **1998**, *108*, 4340–4348.
  - [15] Reith, D.; Meyer, H.; Müller-Plathe, F. *Macromolecules* **2001**, *34*, 2235–2245.
  - [16] Baschnagel, J.; Binder, K.; Doruker, P.; Gusev, A.; Hahn, O.; Kremer, K.; Mattice, W. L.; Müller-Plathe, F.; Murat, M.; Paul, W.; Santos, S.; Suter, U. W.; Tries, V. *Adv. Polym. Sci* **2000**, *152*, 41–156.
  - [17] Lyubartsev, A. P.; Laaksonen, A. *Phys. Rev. E* **1995**, *52*, 3730–3737.
  - [18] Karttunen, M.; Laaksonen, A.; Lyubartsev, A. P.; Vattulainen, I. *submitted* **2002**.
  - [19] Besold, G.; Vattulainen, I.; Karttunen, M.; Polson, J. M. *Phys. Rev. E* **2000**, *62*, R7611–R7614.
  - [20] Vattulainen, I.; Karttunen, M.; Besold, G.; Polson, J. M. *J. Chem. Phys.* **2002**, *116*, 3967–3979.
  - [21] McGreevy, R. L.; Pusztai, L. *Mol. Sim.* **1988**, *1*, 359–367.
  - [22] Reatto, L.; Levesque, D.; Weis, J. J. *Phys. Rev. A* **1986**, *33*, 3451–3465.
  - [23] Rosenfeld, Y.; Kahl, G. *J. Phys.: Cond. Mat.* **1997**, *9*, L89–L98.
  - [24] Gonzalez-Mozuelos, P.; Carbajal-Tinoco, M. D. *J. Chem. Phys.* **1998**, *24*, 11074–11084.
  - [25] Lyubartsev, A. P.; Marcelja, S. *Phys. Rev. E* **2002**, *65*, 041202.
  - [26] Ostheimer, M.; Bertagnolli, H. *Mol. Sim.* **1989**, *3*, 227–233.
  - [27] Soper, A. K. *Chem. Phys.* **1996**, *202*, 295–306.
  - [28] Toth, G.; Baranyai, A. *J. Mol. Liquids* **2000**, *85*, 3–9.
  - [29] Lyubartsev, A. P.; Laaksonen, A. *Chem. Phys. Lett.* **2000**, *325*, 15–21.
  - [30] Swendsen, R. H. *Phys. Rev. Lett.* **1979**, *42*, 859–861.
  - [31] Pawley, G. S.; Swendsen, R. H.; Wallace, D. J.; Wilson, K. G. *Phys. Rev. B* **1984**, *29*, 4030–4040.
  - [32] Groot, R. D.; Warren, P. B. *J. Chem. Phys.* **1997**, *107*, 4423–4435.
  - [33] Forrest, B. M.; Suter, U. W. *J. Chem. Phys.* **1995**, *102*, 7256–7266.
  - [34] Lyubartsev, A. P.; Laaksonen, A. *Phys. Rev. E* **1997**, *55*, 5689–5696.
  - [35] Toukan, K.; Rahman, A. *Phys. Rev. B* **1985**, *B31*, 2643–2648.
  - [36] Smith, D. E.; Dang, L. X. *J. Chem. Phys.* **1994**, *100*, 3757–3766.
  - [37] Lide, D. R., Ed. *CRC Handbook of Chemistry and Physics*; CRC Press: Boca Raton, 82nd ed., 2001.
  - [38] Terämä, E.; Vattulainen, I.; Patra, M.; Karttunen, M.; Lyubartsev, A. P.; Laaksonen, A. *in preparation* **2002**.
  - [39] Lyubartsev, A. P.; Laaksonen, A. *J. Chem. Phys.* **1996**, *100*, 16410–16418.